Authors: Lybaert L., Vanparijs N., Fierens K., Schujs M., Nuhn L., Lambrecht B.N., De Geest B.G.

In: Biomacromolecules 2016, 17(3): 874-881

Lybaert L., Vanparijs N., Fierens K., Schujs M., Nuhn L., Lambrecht B.N., De Geest B.G. (2016) A generic Polymer-Protein Ligation Strategy for Vaccine Delivery. Biomacromolecules 17 874-881
DOI: 10.1021/acs.biomac.5b01571

A generic polymer-protein ligation strategy for vaccine delivery

Lien Lybaert,[1] Nane Vanparijs,[1] Kaat Fierens,[2] Martijn Schuijs,[2] Lutz Nuhn,[1] Bart N. Lambrecht,[2] Bruno G. De Geest[1]*

[1] Department of Pharmaceutics, Ghent University, Ottergemsesteenweg 460, 9000 Ghent, Belgium

[2] VIB Inflammation Research Center, Ghent University, Technologiepark 927, 9052 Ghent Belgium

KEYWORDS Polymers, RAFT, vaccines, dendritic cells

ABSTRACT Although the field of cancer immunotherapy is intensively investigated, there is still a need for generic strategies that allow easy, mild and efficient formulation of vaccine antigens. Here we report on a generic polymer-protein ligation strategy to formulate protein antigens into reversible polymeric conjugates for enhanced uptake by dendritic cells and presentation to CD8 T-cells. A N-hydroxypropylmethacrylamide (HPMA) based co-polymer was synthesized via RAFT polymerization followed by introduction of pyridyldisulfide moieties. To enhance ligation efficiency to ovalbumin, that is used as model protein antigen, protected thiols were introduced onto lysine residues and deprotected *in situ* in presence of the polymer. The ligation efficiency was compared for both the thiol-modified versus unmodified ovalbumin and the reversibility was confirmed. Furthermore the obtained nano-conjugates were tested *in vitro* for their interaction and

association with dendritic cells, showing enhanced cellular uptake and antigen cross-presentation to CD8 T-cells.

1. INTRODUCTION

Dendritic cells (DCs) were first described by Ralph Steinman and co-workers as heterogeneous, large stellate cells that are potent stimulators of the immune system with a much higher antigen presentation capacity compared to other cell subclasses such as macrophages and B-lymphocytes.[1,2] This discovery has led to major insights in how the immune system interacts with foreign material, revealing dendritic cells as the critical factor in the interplay between the innate and the adaptive immune response.[3,4] DCs are the most potent class of antigen presenting cells (APCs) of the immune system and have the capacity to efficiently recognize pathogens, process and present these foreign antigens to T-lymphocytes leading to activation and proliferation of adaptive immune responses.[5,6] Presentation of antigens on the cell surface of DCs is mediated by major histocompatibility complex (MHC) peptides, either MHC-I or MHC-II. Intracellular antigens are normally restricted to MHC-I presentation and can activate cytotoxic $CD8^+$ T-cells (CTLs) or killer T-cells whereas extracellular antigens are presented via the MCH-II class inducing $CD4^+$ T-cells or T-helper cells.[7-9]

However, DCs are also able to present extracellular antigens via MHC-I, through a process called cross-presentation.[10,11] CTLs can recognize and eliminate malignancies by release of proteases, i.e. perforins and granzymes.[13,14] Therefore cancer immunotherapy, focusing on stimulating DCs with tumor-associated antigens[15-18] is a promising strategy that aims for harnessing the patient´s immune system without facing the ubiquitous side effects of chemo- and radiotherapy[3,12] In this regard, formulating protein antigens into particulate carriers is highly attractive as this dramatically

promotes cross-presentation relative to soluble antigens.[15,19-22] Sub-micron particles are preferred over bigger ones due to their higher tissue mobility and by consequence ability to target different DC subsets. On the one hand, peripheral migratory DCs can recognize and take up particles at their injection site followed by lymphatic transport to the lymph nodes and antigen-presentation to T-cells. On the other hand, only small nanoparticles, in the sub 200 nm range, will additionally drain to the lymph nodes via passive diffusion into the lymphatics and also target lymph-node resident DCs.[23-26]

In this paper we report on a generic strategy for the formulation of antigens into nano-scaled polymeric conjugates based on co-polymers of N-hydroxypropyl methacrylamide (HPMA) with 3-aminopropyl methacrylamide (APMA). The neutral hydrophilic HPMA moieties provide water solubility and biocompatibility.[27-29] Additionally, the APMA units will be used to introduce pyridyldisulfide moieties for reversible protein conjugation via disulfide formation and enhancement of cell uptake by interaction with exofacial thiols.[30, 31] **Figure 1** shows a schematic representation of the concept.

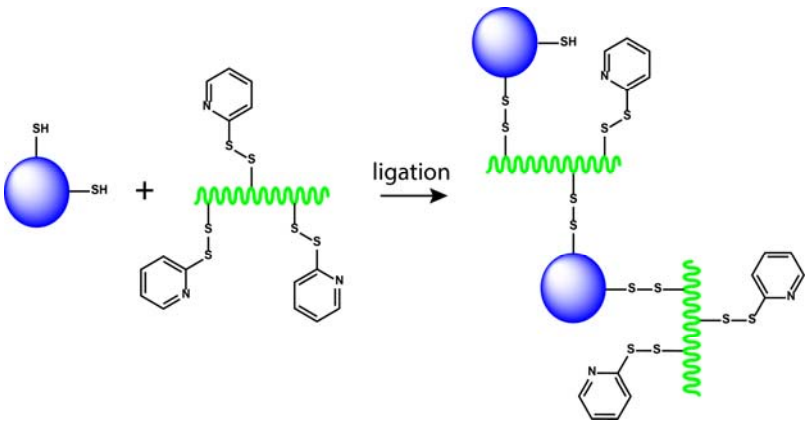

Figure 1. Schematic illustration of generic polymer-protein ligation strategy based on reversible disulfide formation between free thiols on a protein and pyridyldisulfide moieties on a polymer

backbone. A mixture is obtained composed of multiple polymers per protein and/or multiple proteins per polymer.

2. EXPERIMENTAL METHODS

2.1 Materials. Hydroxypropyl methacrylamide (HPMA) and aminopropyl methacrylamide (APMA) were obtained from Polysciences. Anhydrous acetic acid was purchased from Biosolve chemicals. Dimethylsulfoxide (DMSO), mercapto-propanoic acid, 4-cyanovaleric acid dithiobenzoate (CTP), 4,4'-azobis(4-cyanovaleric acid) (ACVA), basic alumina, 3-(4,5-dimethylthiazol-2-yl)-2,5-diphenyltetrazolium bromide (MTT) reagent, sodium dodecyl sulfate (SDS), ethanol, dichloromethane, Na_2EDTA, hydroxylamine Atto 647N NHS ester, $NaHCO_3$, paraformaldehyde and PD10 desalting columns were obtained from Sigma Aldrich. Phosphate buffered saline pH 7,2 (PBS), RPMI-glutamax 1640 medium, fetal bovine serum EU qualified (FBS), penicillin/streptomycin (5000 U/mL), sodium pyruvate (100mM), cell dissociation buffer (PBS based), Hoechst and cholera toxine B conjugates to AlexaFluor555 (CTB-AF555) were purchased from Invitrogen. Dipyridyldisulfide (DPDS) and 4-(4,6-Dimethoxy-1,3,5-triazin-2-yl)-4-methylmorpholinium Chloride (DMTMM) were obtained from TCI America. 2-Mercaptoethanol, Laemli sample buffer (4x), Coomassie blue stain (G-250) and the 4-20 % mini-protean TGX gels were purchased from Bio-rad. S-acetylthiopropionate N-succinimidyl ester (SATP), TNBSA solution and hydrochloric acid (HCl) 37% v/v were obtained from Thermo Scientific whereas the pre-treated Spectra/Por 7 dialysis membranes were purchased from Spectrumlabs.

2.2 Instrumentation.

^{1}H-Nuclear magnetic resonance (NMR). NMR spectra were recorded on a Bruker 300 MHz FT NMR in D_2O and d_6-DMSO. Chemical shifts (δ) are provided in ppm relative to TMS.

Size exclusion chromatography (SEC). SEC elugrams were recorded on a Shimadzu 20A system in dimethylacetaminde (DMAc) as solvent containing 50 mM LiBr. The system was equipped with a 20A ISO-pump and a 20A refractive index detector (RID). Measurements were recorded at 50 °C with a flow rate of 0.7 mL/min. Calibration of the 2 PL 5 μm Mixed-D columns was done with polymethylmethacrylate (PMMA) standards obtained from PSS (Mainz, Germany).

Electron spray ionization-mass spectroscopy (ESI-MS). ESI-MS was carried out on a Waters LCT Premier XETM TOF mass spectrometer with a ZsprayTM source, ESI and modular LocksprayTM interface, coupled to a Waters alliance HPLC system.

UV-VIS spectrophotometry. UV-VIS spectra were recorded on a Shimadzu UV-1650PC spectrophotometer in 1 cm x 1 cm quartz cells.

Dynamic light scattering (DLS). DLS analyses were performed on a Zetasizer Nano S (Malvern Instruments Ltd., Malvern, U.K.) with a HeNe laser (λ = 633 nm) at a scattering angle of 173°.

2.3 Synthesis of poly(HPMA-co-APMA). Based on Qin *et al.*[32] a copolymer composed of hydroxypropyl methacrylamide and aminopropyl methacrylamide (HPMA-co-APMA) was synthesized via aqueous reversible addition-fragmentation chain transfer (RAFT) polymerization using 4,4'-azobis(4-cyanovaleric acid) as the initiator and 4-cyanovaleric acid dithiobenzoate as the RAFT agent. The RAFT polymerization was set for a HPMA/APMA ratio of 80/20 and a target degree of polymerization (DP) of 100. After dissolution of HPMA (3.491 M), APMA (0.873 M) and ACVA (0.218 M) in deionized water CTP, dissolved in 1,4-dioxane, was added in a final concentration of 0.436 M. Subsequently, oxygen was removed via four cycles of freeze-pump-

thaw. The polymerization was initiated by heating the mixture to 70 °C in an oil bath for 24 h. Purification of the co-polymer was achieved by precipitation in acetone followed by removal of residual solvent via vacuum pump (24 h). Confirmation of the co-polymerization was assessed by ^{1}H NMR analysis and the DP was determined by GPC analysis. Conversion rate of the RAFT polymerization was achieved by ^{1}H NMR analysis of the reaction mixture at different time points. ^{1}H NMR peak assignment (300 MHz, D_2O): δ (ppm) 0.99-1.20 ($CH_2CH(OH)C\mathit{H}_3$, $CH_2C(C\mathit{H}_3)CO$), 1.80-1.92 ($C\mathit{H}_2C(CH_3)$-CO, $CH_2C\mathit{H}_2CH_2NH_2$), 3.08 ($CH_2CH_2C\mathit{H}_2NH_2$), 3.24 ($CONHC\mathit{H}_2CH(OH)CH_3$, $CONHC\mathit{H}_2CH_2CH_2NH_2$), 3.94 ($CH_2C\mathit{H}$-$(OH)CH_3$).

2.4 Synthesis of PDPA. Based on Hugh *et al.* 3-(2-pyridyldithio)-propanoic acid (PDPA) was synthesized.[33] In brief, 3-mercapto-propanoic acid (0.0249 mmol) was added to a 0.623 M solution of 2,2'-dipyridyldisulfide (DPDS) in anhydrous ethanol in the presence of acetic acid. The solution was subsequently stirred for 2 hours at room temperature. Purification of PDPA was assessed by basic alumina column chromatography using a 3:2 mixture of dichloromethane and ethanol followed by elution of PDPA via addition of 4 % of acetic acid to the eluent mixture. Traces of acetic acid were removed under high vacuum for 48 h. The synthesis and purity of the product was confirmed by ^{1}H NMR analysis and LC-MS (ESI^+) analysis. ^{1}H NMR peak assignment (300 MHz; d_6-DMSO): δ (ppm) 2.59 (2H, t, J = 7.0), 2.98 (2H, t, J = 7.0), 7.23 (1H, ddd, J = 7.1, 4.8, 1.2), 7.75 (1H, d, J = 8.0), 7.8 (1H, td, J = 7.9, 1.4), 8.4 (1H, d, J = 4.9), 12.43 (1H, broad s). Theoretical mass of PDPA: 215.01 and experimental mass: ESI+ m/z in MeOH – 216.0 (MH+).

2.5 Synthesis of poly(HPMA-PDS). To a 5 mg/mL solution of poly(HPMA-co-APMA) in a phosphate buffered saline (PBS) 1.5 M excess of DMTMM was added followed by an equimolar amount of PDPA dissolved in DMSO. The reaction was stirred overnight for 24 h at room

temperature followed by purification via dialysis against deionized water (MWCO 3.5 kDa) for 24 h and lyophilization. The synthesis was confirmed via ^{1}H NMR analysis.

2.6 Cell lines. The DC2.4 cell line was a kind gift from Dr. Kenneth Rock (University of Massachusetts, Boston, US).[34] DC2.4 cells were cultured in RPMI-glutamax medium supplemented with 10 % fetal bovine serum, 1 % penicillin/streptomycin and 1 mM sodium pyruvate and incubated at 37 °C with 5 % CO_2 saturation. Isolation of the cells for experiments was performed by incubation of the cells in a PBS-based dissociation buffer for 10 minutes.

2.7 MTT assay

Cell toxicity was measured by seeding DC2.4 in 96 well plates at a density of 50000 cells/mL in complete RPMI medium (total volume 100 µL) 1 day prior to addition of increasing concentrations of poly(HPMA-co-APMA) in PBS. Subsequently the cells were cultured for 24 h followed by addition of 40 µL of the MTT reagent (1 mg/mL). After an incubation period of 2-3 h the formed formazan crystals were dissolved in 100 µL of a 10 % m/v SDS/0.01 M HCl solution overnight protected from light. The absorbance was measured by a microplate reader at 570 nm. As a negative and positive control PBS buffer and DMSO respectively were added to the wells.

2.8 Synthesis of OVA-SATP. Protected thiol groups were introduced via interaction with SATP. First a 120 µM solution of ovalbumin (OVA) was prepared in PBS pH 7,2. Second, SATP dissolved in dry DMSO was added in different molar ratios of SATP to OVA, i.e. 1:5, 1:10, 1:20, 1:50. After incubation of 45 min at room temperature the unreacted fraction was eliminated via a disposable PD10 column. The pure fractions of protein were distinguished from the waste fractions by UV spectrophotometry followed by lyophilization. Quantification of the introduced thiol percentage was assessed by the trinitrobenzene sulfonic acid assay(TNBSA) preceded by

deprotection of the thiols in a deacetylation PBS buffer pH 7,2 containing 0.05 M hydroxylamine and 0.025 mM Na_2EDTA.

2.9 TNBSA

The residual amine content of OVA after SATP substitution was determined by the (2,4,6-trinitrobenzene sulfonic acid assay (TNBSA) according to the manufacturers' instructions. First OVA and OVA-SATP were dissolved in a 0.1 M sodium bicarbonate buffer pH 8.5 at 50 μg/mL followed by addition of 0.25 mL of a 0.01 % TNBSA solution to 0.5 mL of each sample. After incubation of 2 hours at 37 °C 0.25 mL 10 % SDS and 0.125 mL 1 N HCl were added. Subsequently, absorbance was measured at 335 nm.

2.10 Polymer-protein conjugation. To a 0.465 M OVA solution in deacetylation buffer different molar polymer:OVA ratios were added to a final volume of 1 mL in PBS. The molar ratios used were 1:1, 2:1, 2.5:1, 3:1 and 4:1. The reaction was incubated for 2 hours at room temperature followed by visualization of the conjugation efficiency via SDS-PAGE and semi-quantitative analysis of the encapsulation via Image J.

2.11 Gel electrophoresis (SDS-PAGE). To analyze protein conjugation or to determine the reversibility of the synthesized particles, gel electrophoresis was performed. The samples were diluted with respectively Laemli sample buffer solution (4x) or with a 1:9 2-mercaptoethanol:Laemli sample buffer solution (4x), incubated for 5 minutes at 95 °C and loaded on 4-20 % precast gels. After the run (150 kV), visualization of the protein bands was achieved by incubation of the gels into Coomassie blue stain.

2.12 Fluorescent labeling. The remaining unsubstituted APMA units of poly(HPMA-PDS) were labeled with the Atto647-NHS ester according to the manufacturers' instructions. In brief, the

fluorescent dye was dissolved in dry DMSO (2.3 mM) and added to a 5 mg/mL polymer solution in 0.1 M $NaHCO_3$ buffer (pH 8.3) aiming a target degree of 2.5 %. After incubation of 30 to 60 minutes protected from light at room temperature the excess was removed via PD10 column purification followed by lyophilization. Second, the fluorescent conjugates were synthesized as described above using the fluorescently labeled poly(HPMA-PDS) and a molar ratio of OVA:OVA-AF488 49:1. After 2 h incubation the particles were dialyzed against deionized water for 48 h (MWCO 100 kDa).

2.13 In vitro DC2.4 uptake assay. DC 2.4 cells were seeded at a density of 0.4 x 10^6 cells/mL in a 24 well plate one day prior to the addition of the fluorescent particles at different concentrations. After 24 h incubation the cells were dissociated using cell dissociation buffer followed by centrifugation for 5 min at 200 G at 0 °C. After resuspension, the samples were stored on ice and measured by the BD Accuri C6 flow cytometer. The data was analyzed using FlowJo.

2.14 Confocal microscopy imaging. DC2.4 cells were seeded at a density of 0.2 x 10^6 cells/mL in a glass bottom Will-co dish and incubated overnight. Next, the fluorescent particles were added, incubated for 24 h and fixated in a 2 % paraformaldehyde solution for 10-15 minutes. The cells were subsequently washed and simultaneously stained by CTB-AF555 and Hoechst for 1 h at room temperature. Finally the samples were washed with PBS and visualized by confocal microscopy. This was carried out on a Leica DMI6000 B inverted microscope equipped with an oil immersion objective (Zeiss, 63×, NA 1.40) and attached to an Andor DSD2 confocal scanner. Images were processed with ImageJ.

2.15 In vitro OT-I proliferation assay and ELISA. Mouse bone marrow derived DCs (bmDCs) were isolated by flushing femurs of C57BL/6 mice with complete RPMI with a 26G needle. The

cell suspension was filtered through a 100 μm cell strainer and incubated for 3-5 minutes in red blood cell lysis buffer on ice. The cells were subsequently seeded into a 24 well plate at a density of 3 x 10^5 cells/mL in complete RPMI containing 20 ng/mL of GM-CSF and incubated at 37°C/5% CO_2 for 7 days. To ensure optimal bmDC growth, fresh medium containing 20 ng/mL GM-CSF was added on day 3 and on day 6 the medium was refreshed. On day 7 the bmDCs were isolated and pulsed with the test compounds containing 0.2, 2 and 5 mg/mL OVA followed by co-culture with CFSE-labeled OVA specific transgenic CD8 T-cells, according to previously described protocols.[35]

3. RESULTS AND DISCUSSION

3.1 Synthesis and modification of poly(HPMA-co-APMA).

Co-polymerization of HPMA and APMA was performed by reversible addition-fragmentation transfer (RAFT) polymerization according to Zhu Qin *et al.*[32] for a targeted degree of polymerization (DP) of 100 repeating units (corresponding to a target molecular weight of 14 kDa) composed of 80 HPMA repeating units and 20 APMA repeating units. Being a controlled radical polymerization technique, RAFT yields access to polymers with a well-defined chain length and a low dispersity[36,37], which is of interest to obtain polymers with a molecular weight below the renal clearance threshold that can be eliminated from the body. ^{1}H NMR analysis indicated a conversion of 76 % and a composition of 80% HPMA and 20 % APMA, which is in good accordance to the monomer composition (**Figure 2A**). A low dispersity of 1.08 and a M_n of 16 kDa was obtained via size exclusion chromatography (SEC) in dimethylacetamide.

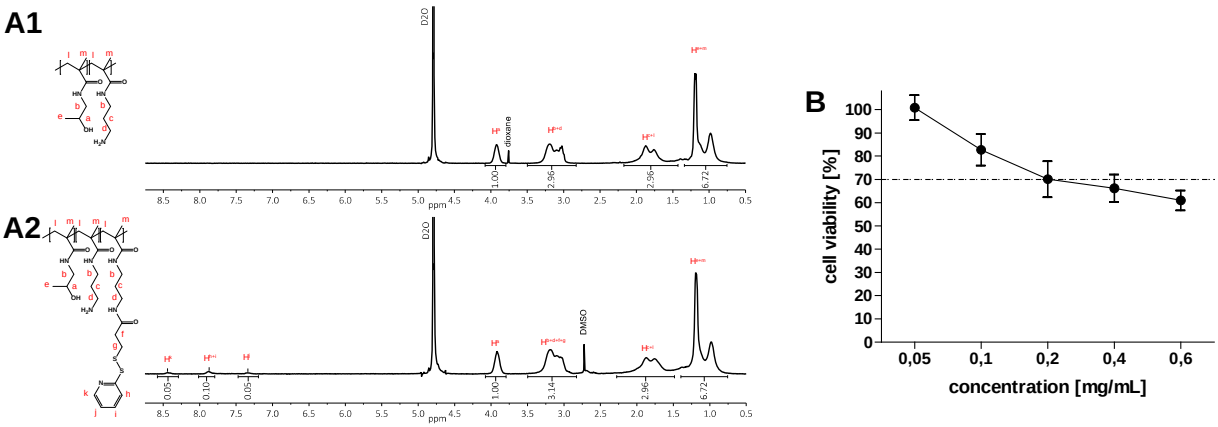

Figure 2. (A1) ^{1}H-NMR spectrum of poly(HPMA-co-APMA) and (A2) ^{1}H-NMR spectrum of poly(HPMA-PDS) (B) *In vitro* MTT cytotoxicity assay of poly(HPMA-co-APMA) on DC2.4 cells.

Subsequently we engineered antigen-binding properties into the polymers (**Figure 3A**). First, we synthesized 3-(2-pyridyldithio)-propanoic acid (PDPA) by thiol-disulfide exchange of 2,2-dipyridyldisulfide and 3-mercapto propionic acid in the presence of acetic acid, based on Hugh *et al.*[33] Secondly, the APMA moieties were substituted with PDPA using 4-(4,6-dimethoxy-1,3,5-triazin-2-yl)-4-methylmorpholinium chloride (DMTMM) as amidation reagent to introduce pending pyridyldisulfide moieties onto the poly(HPMA) backbone. ^{1}H-NMR spectroscopy revealed a degree of substitution of 20 % of the primary amine moieties. This polymer will be further denoted as poly(HPMA-PDS) (**Figure 2B**). The latter can undergo disulfide exchange with free thiols present on cysteine residues of proteins and pyridyldisulfide based protein conjugation strategies have widely been explored in combination with RAFT polymerization.[38-42] Indeed, disulfides are attractive moieties for designing drug delivery systems. Firstly, they are readily formed with free thiols of cysteine residues. Secondly, disulfides are stable under (oxidative) extracellular conditions but can be reduced to free thiols in the cytoplasm of cells. Third, disulfide

exchange with cell surface thiols can enhance cellular uptake and can also trigger dissociation of disulfides.[30, 31] The potential cytotoxicity of the residual amine groups on the poly(HPMA-PDS), was assessed by the MTT (3-(4,5-dimethylthiazol-2-yl)-2,5-diphenyltetrazolium bromide) cell viability assay on the immortalized DC2.4 cell line for increasing concentrations of poly(HPMA-co-APMA). As shown in **Figure 2B**, up to a polymer concentration of 0.2 mg/mL, no cytotoxicity is observed, evinced by a cell viability above 70%. In further experiments polymer concentrations well below this threshold (concentration range between 0.0011 mg/mL-0.017 mg/mL) were used to ensure optimal cell viability during these experiments.

3.2 Antigen modification with protected thiols.

Antigen conjugation to poly(HPMA-PDS) requires the presence of free thiols on the protein backbone for thiol-disulfide exchange with the PDS moieties. As the composition of every protein differs, variable conjugation efficiency is likely for every other antigen. In addition, it is possible that the amount of thiols per protein will not be sufficient to afford efficient formulation of the respective antigen into nano-conjugates. Therefore we opted to generalize the conjugation strategy. In this regard, we introduced protected thiols onto lysine residues that are more abundantly present on proteins than cysteines. As a model protein antigen we used ovalbumin (OVA) because the latter contains peptide sequences that are recognized by the murine immune system as CD4 and CD8 epitopes. Moreover, a wide variety of *in vitro* and *in vivo* tools are available for immunological assessment of OVA based vaccine formulations. OVA was reacted with a molar ratio of OVA to S-acetylthiopropionate N-succinimidyl ester (SATP) of 1 to 15. This compound substitutes primary amines on lysine residues with acetylated thiols that can be deprotected *in situ*

in presence of hydroxylamine (**Figure 3B**), and subsequently undergo disulfide exchange with poly(HPMA-PDS). The decrease in free amines was quantified by spectrophotometry using the (2,4,6-trinitrobenzene sulfonic acid) assay (TNBSA), thereby indicating 78 % of all available lysines to be substituted (**Figure 3C**).

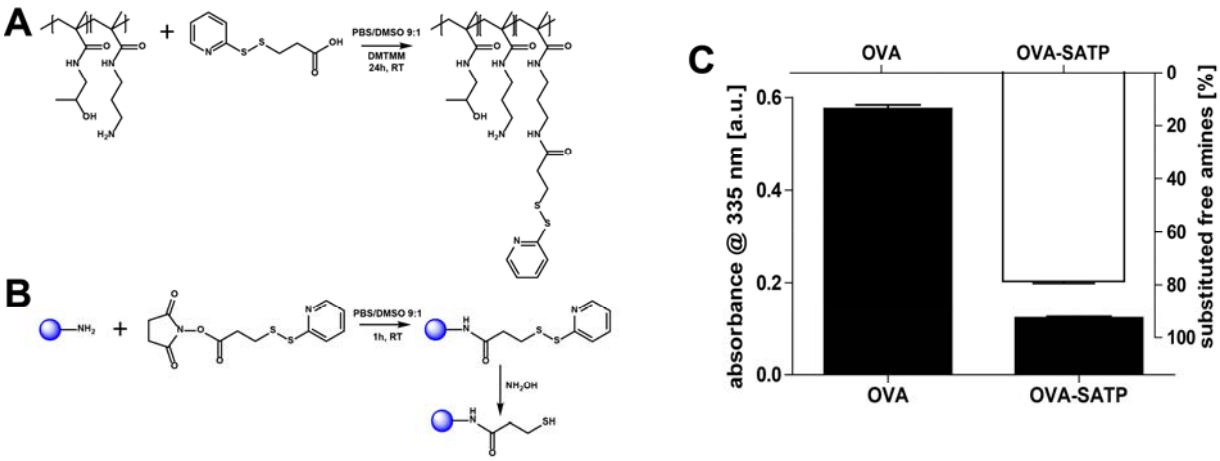

Figure 3. (A) Modification of poly(HPMA-co-APMA) with PDPA (B) Substitution of lysine residues with SATP and subsequent deprotection to free thiols (C) Determination of the extent of OVA modification with SATP determined by TNBSA assay.

3.3 Antigen conjugation.

In a first series of experiments, the polymer-conjugation efficiency of OVA-SATP was compared versus unsubstituted OVA. SDS-PAGE was used to assess protein conjugation of poly(HPMA-PDS) to OVA and OVA-SATP. For unsubstituted OVA, no difference could be observed upon incubation of the protein with the polymer. In contrast, the free OVA band disappears almost completely when OVA-SATP is used as shown in **Figure 4**. This confirms that SATP substitution

strongly increases the polymer-protein conjugation efficiency. Interestingly three distinct bands appear that correspond either to OVA that is ligated to several polymer strands or *vice versa*, along with a broad spread of higher molecular weight bands. These data suggest that besides polymers being grafted onto the protein, also polymeric crosslinking among different proteins occur. Dynamic light scattering (DLS; **Figure 4B**) revealed the presence of small conjugates without extensive inter-particle crosslinking, as evidenced by both the size distribution and the correlation curves. This property is of importance with regard to tissue mobility *in vivo*.

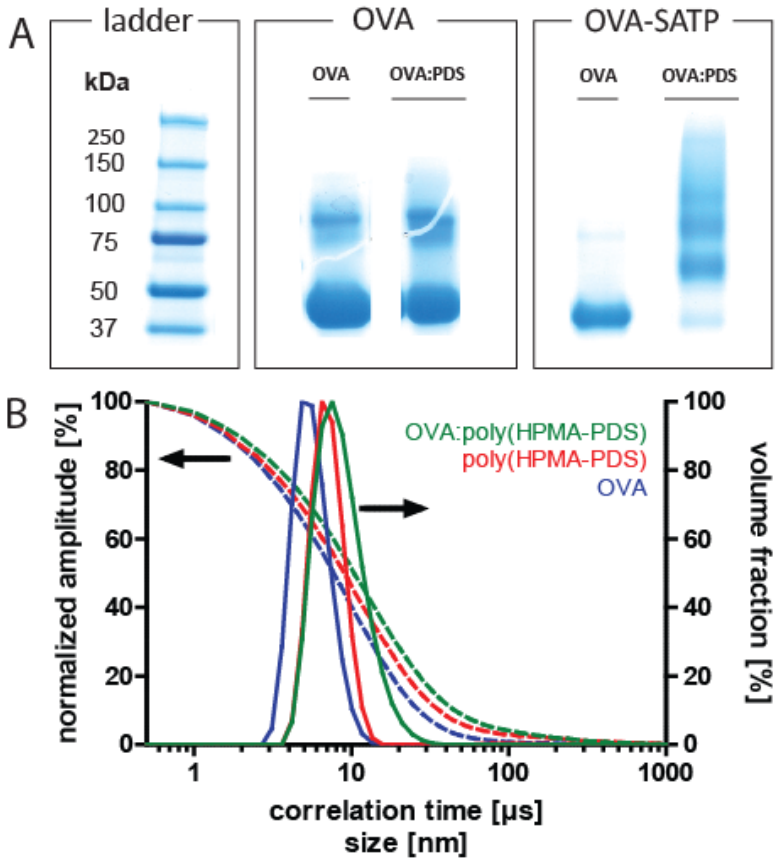

Figure 4. (A) SDS-PAGE analysis of OVA and OVA-SATP ligated to poly(HPMA-PDS) in a 1:1 molar ratio. (B) DLS data of soluble OVA, poly(HPMA-PDS) and the OVA:poly(HPMA-PDS).

The required ratio of polymer to OVA-SATP to yield optimal conjugation was determined by visualization of the conjugation efficiency of different molar ratios of OVA-SATP to poly(HPMA-PDS), by SDS-PAGE. **Figure 5** indicates that approximately 100% conjugation can be already obtained at an equimolar ratio of OVA-SATP to poly(HPMA-PDS). Therefore, we decided to use a ratio of OVA to polymer of 1:1 in further experiments. To assess the reversible nature of the disulfide bonds formed between OVA-SATP and the poly(HPMA-PDS), SDS-PAGE was performed in presence and absence of 2-mercaptoethanol as a reducing agent. As shown in **Figure 5**, in presence of 2-mercaptoethanol, the band corresponding to OVA-SATP reappears again as a single protein band confirming the reversibility of the conjugation.

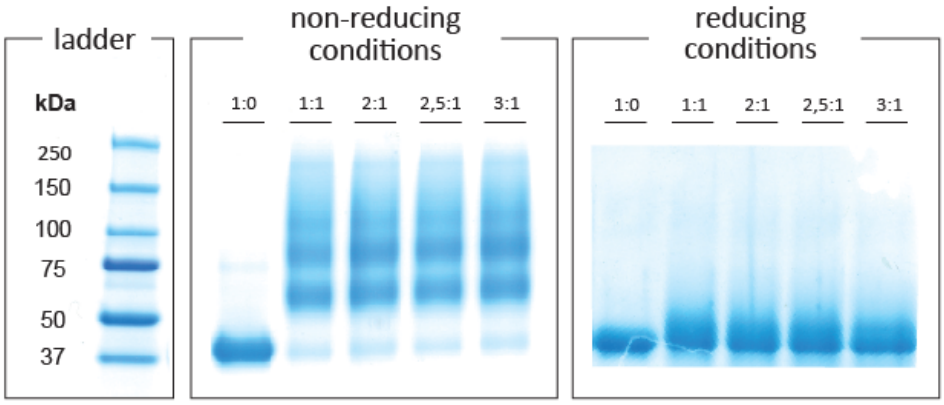

Figure 5. SDS-PAGE analysis of OVA-SATP to poly(HPMA-PDS) conjugation for varying protein to polymer ratios. Gel electrophoresis was performed under non-reducing and reducing (presence of 2-mercaptoethanol) conditions to investigate the reversibility of the conjugation.

3.4 In vitro characterization.

Next we aimed at investigating the effect of polymer conjugation on the uptake of OVA by DCs. First, poly(HPMA-PDS) was fluorescently labeled with Atto647 NHS ester and conjugated to AlexaFluor488-labeled OVA (OVA-AF488) to allow analysis of the uptake of both OVA and the respective polymer. The resulting conjugates were incubated in different concentrations overnight at 37°C with DC2.4 cells (an immortalized murine dendritic cell line).[36] Flow cytometry analysis of the mean AF488 fluorescence per cell (**Figure 6A1**), showed a dose-dependent cellular association of the antigen and indicates that poly(HPMA-PDS) conjugation leads, relative to soluble OVA, to higher uptake efficiency of OVA. A similar dose-dependent trend was observed for the mean Atto647 fluorescence per cell for poly(HPMA-PDS) (**Figure 6A2**). This data indicates that both OVA and the polymer associate with the dendritic cells.

To investigate whether the conjugates are internalized by the DCs or merely bound to the cell surface, confocal microscopy was performed. **Figure 6B** reveals that the conjugates are indeed internalized by the DCs. The co-localizing signals of OVA-AF488 and of the polymer-Atto647 inside the cells also confirms that, upon uptake of the conjugates, the polymers are trafficked within the same intracellular vesicles as OVA and the conjugates are not cleaved at the cell surface.

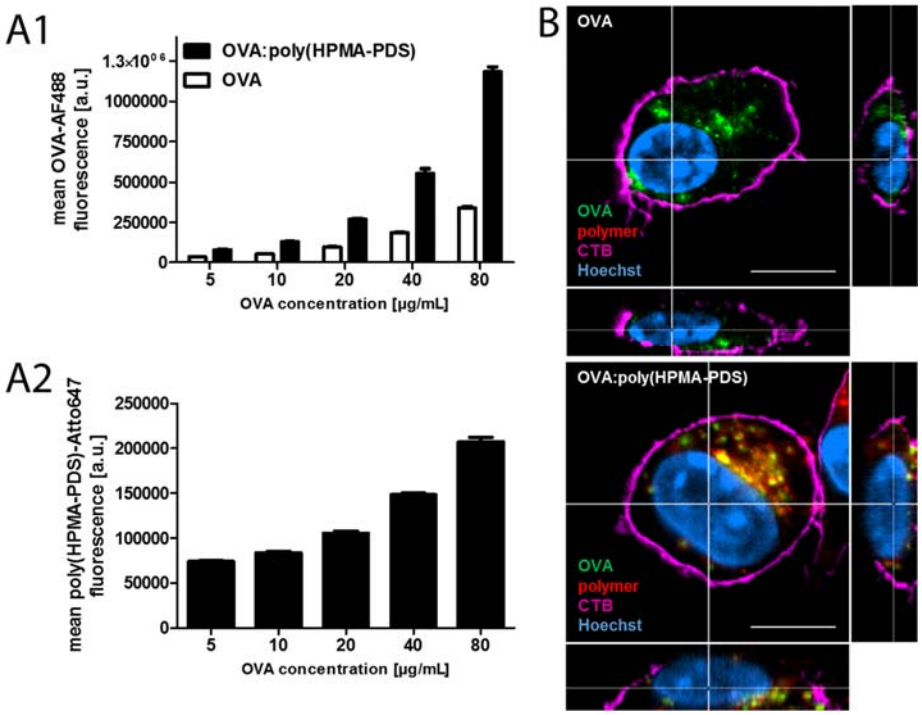

Figure 6. *In vitro* interaction of dendritic cells with OVA and OVA:poly(HPMA-PDS). (A) Flow cytometry analysis of the interaction of DCs with OVA (A1) and with poly(HPMA-PDS) (A2), as function of OVA concentration. (B) Confocal microscopy images. Cell membrane is stained with AF555-labeled cholera toxin B (CTB-AF555). Cell nuclei are stained with Hoechst. Scale bar represents 15 µm.

To identify the reason for which polymer-conjugated OVA shows higher uptake than soluble OVA, we pulsed DCs with soluble OVA and poly(HPMA-PDS) separately at 4°C. Under these conditions, energy dependent uptake mechanisms are blocked. As shown in **Figure 7A**, soluble OVA is not associated with the DCs at 4°C, opposed to poly(HPMA-PDS) which does show dose-dependent cellular association. Confocal microscopy (**Figure 7B**; overlaying the DIC and the Atto647 channel) confirmed that at 4°C, poly(HPMA-PDS) is indeed bound to the cell membrane.

Taken together, we hypothesize that remaining pyridyldisulfide moieties on the conjugates promote interaction with cysteine residues of cell surface proteins and thereby bind to the cell membrane [29, 30].

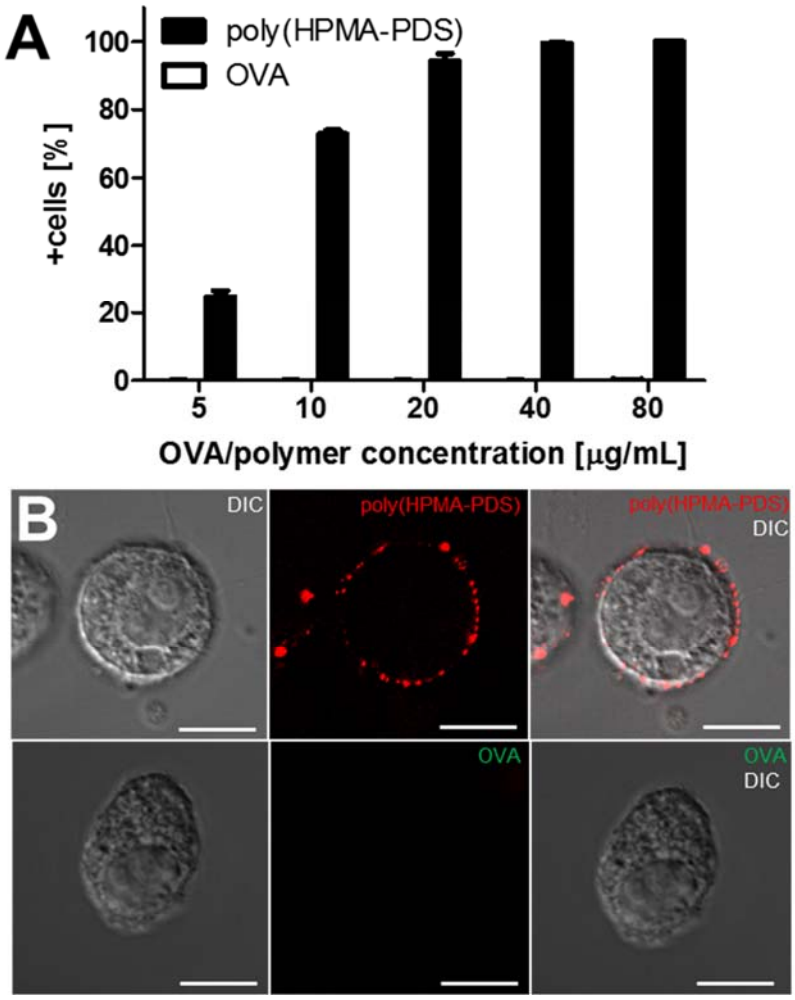

Figure 7. Investigation of energy independent cellular association of DCs pulsed with soluble OVA and poly(HPMA-PDS) at 4°C. (A) Flow cytometry analysis (B) Confocal microscopy images. Scale bar is 15 μm.

3.5 Immuno-biological evaluation.

Taking into account the high efficiency of OVA conjugation to poly(HPMA-PDS) together with the high uptake efficiency by DCs and the reversibility of the conjugation, we found the poly(HPMA-PDS) based system to have potential for the formulation of protein vaccine antigens.

To assess the immunological potential of the conjugates we determined whether or not poly(HPMA-PDS) conjugation enhances cross-presentation by DCs to CD8 T-cells via an *in vitro* CD8 T-cell proliferation assay. Mouse bone marrow derived dendritic cells (bmDCs) were isolated, pulsed with soluble OVA and OVA:poly(HPMA-PDS) in three different OVA concentrations (0.2, 2 and 5 mg/mL) followed by co-culture with OT-I cells. OT-I cells are CD8 T-cells that express the transgenic T-cell receptor that specifically recognizes the CD8 epitope of OVA (i.e. SIINFEKL) presented via MHC-I. These OT-I cells were labeled with the fluorescent label CFSE in order to allow monitoring of the CD8 T-cell proliferation via flow cytometry analysis. Upon division of the OT-I cells, the fluorescent CFSE marker will be equally divided into the daughter cells leading to a decrease of the fluorescent signal. **Figure 8A** demonstrates that the OVA:poly(HPMA-PDS) conjugates enhance CD8 T-cell proliferation over soluble OVA as evinced by a more pronounced decrease of the CFSE signal. Additionally, ELISA was performed to determine the amount of IFNy that is produced by the CD8 T-cells. IFNy is a pro-inflammatory cytokine that is highly upregulated upon activation of the OT-I cells and drives the effector T-cell response. As depicted in **Figure 8B** the IFNy production is indeed higher when CD8 T-cells are co-cultured with bmDCs that are pulsed with the OVA:poly(HPMA-PDS) conjugates compared to soluble OVA confirming the data obtained by the T-cell proliferation assay.

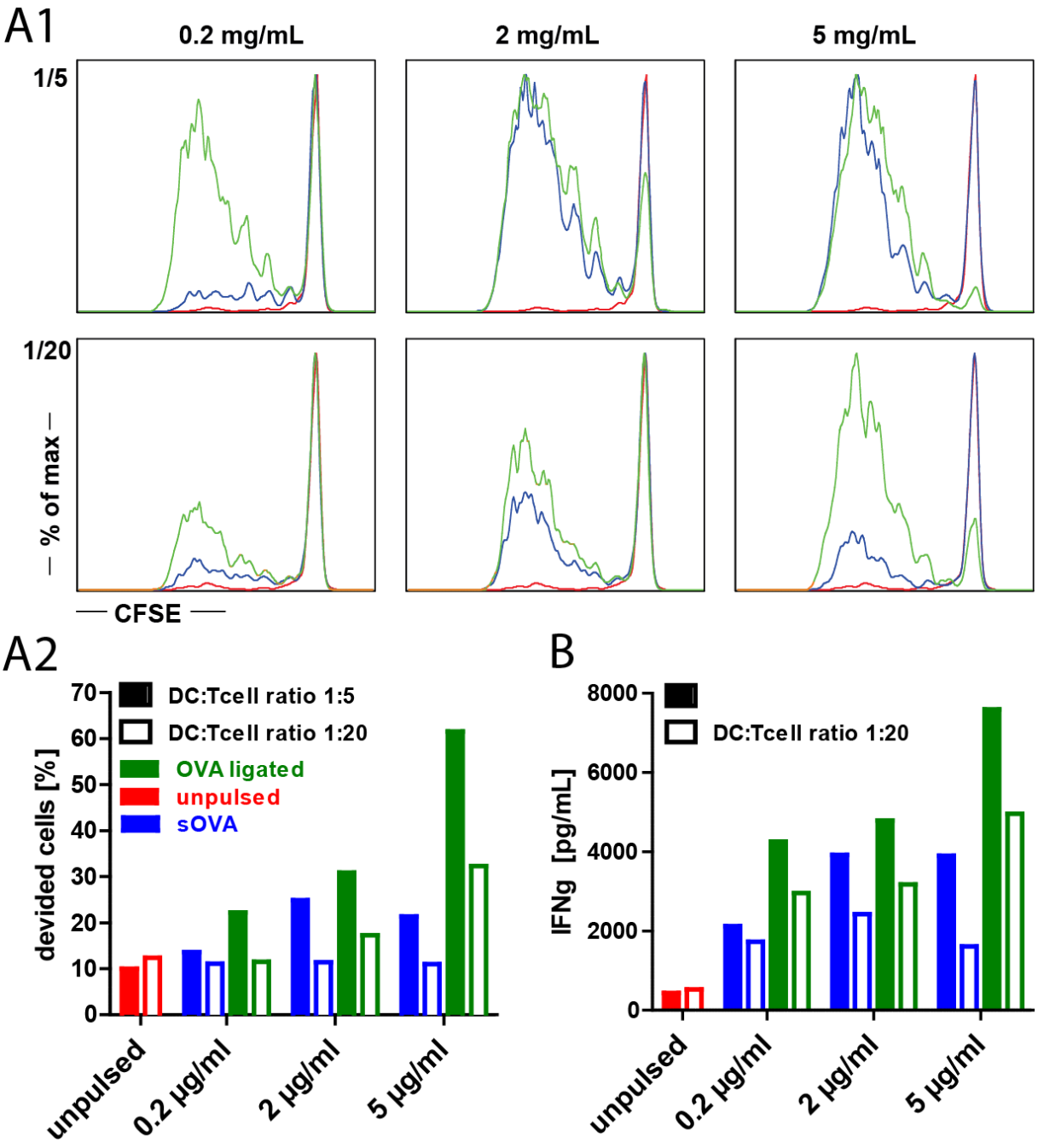

Figure 8. *In vitro* immuno-biological evaluation. (A1) Flow cytometry histograms of CFSE labeled transgenic OT-I OVA-specific CD8 T-cells co-cultured with bmDCs pulsed with different concentrations of OVA and OVA:poly(HPMA-PDS) respectively. BmDC to T-cell ratios of 1/5 and 1/20 were used (A2) Corresponding quantification of T-cell proliferation expressed as the

percentage of divided labeled transgenic OT-I OVA-specific CD8 T-cells. (B) IFNγ secretion in the supernatant of the bmDC/T cell co-cultures measured by ELISA.

4. CONCLUSIONS

To summarize, we have shown in this work that water-soluble HPMA-based RAFT polymers with multiple pending pyridyldisulfide moieties are well suited for protein conjugation, on the condition that these proteins are modified with protected thiols that can be deprotected *in situ*. The obtained conjugates are stable in aqueous medium and can be disassembled in response to reducing conditions. *In vitro* experiments on dendritic cells show that the polymer conjugation of a model antigen resulted in an increased cellular uptake, relative to unconjugated protein, which we attribute to thiol-disulfide exchange between remaining pyridyldisulfide moieties and exofacial thiols present on the cell surface. Furthermore, we demonstrate that polymer conjugation increases antigen presentation by bmDCs to CD8 T-cells *in vitro*. In future research, the effect of polymer conjugation on lymphatic antigen transportation and *in vivo* immune activation will be studied as well as conjugation of molecular adjuvants to these polymers.

AUTHOR INFORMATION

Corresponding Author

*E-mail: br.degeest@ugent.be

Author Contributions

All authors have given approval to the final version of the manuscript.

Funding Sources

This work was financially supported by the Agency for Innovation by Science and Technology in Flanders (IWT) and FWO Flanders.

ACKNOWLEDGMENT

BDG, KF and BNL acknowledge the FWO for funding.

REFERENCES

(1) Steinman, R.M.; Witmer, M.D. *Proc Natl Acad Sci USA*, **1978**, 75, 5132-5136.

(2) Steinman, R.M.; Cohn, Z.A. I. *J Exp Med*, **1973**, 137, 1142-1162.

(3) Palucka, K.; Banchereau, J. *Nat Rev Cancer*, **2012**, 12, 265-277.

(4) Clark, R.; Kupper, T. *J Investig Dermatol*, **2005**, 125, 629-637.

(5) Steinman, R.M.; Banchereau, J. *Nature*, **2007**, 449, 419-426.

(6) Moser, M.; Murphy, K.M. *Nat Immunol*, **2000**, 1, 199-205.

(7) Jensen, P.E. *Nat Immunol*, **2007**, 8, 1041-1048.

(8) Raychaudhuri, S.; Rock, K.L. *Nat Biotechnol*, **1998**, 16, 1025-1031.

(9) Banchereau, J.; Steinman, R.M. *Nature*, **1998**, 392, 245-252.

(10) Joffre, O.P.; Segura, E.; Savina, A.; Amigorena, S. *Nat Rev Immunol*, **2012**, 12, 557-569.

(11) Ackerman, A.L.; Cresswell, P. *Nat Immunol*, **2004**, 5, 678-684.

(12) Aly, H.A. *J Immunol Methods*, **2012**, 382, 1-23.

(13) Appay, V.; Douek, D.C.; Price, D.A. *Nat Med*, **2008**, 14, 623-628.

(14) Boudreau, J.E.; Bonehill, A.; Thielemans, K.; Wan, Y *Mol Ther*, **2011**, 19, 841-853.

(15) Foged, C.; Hansen, J.; Agger, E.M. *Eur J Pharm Sci*, **2012**, 45, 482-491.

(16) Palucka, A.K.; Ueno, H.; Fay, J.W.; Banchereau, J. *Immunol Rev*, **2007**, 220, 129-150.

(17) Palucka, K.; Banchereau, J. *Immunity*, **2013**, 39, 38-48.

(18) Radford, K.J.; Tullett, K.M.; Lahoud, M.H. *Curr Opini Immunol*, **2014**, 27, 26-32.

(19) Joshi, M.D.; Unger, W.J.; Storm, G.; van Kooyk, Y.; Mastrobattista, E. *J Control Rel*, **2012**, 161, 25-37.

(20) Xiang, S.D.; Scholzen, A.; Minigo, G.; David, C.; Apostolopoulos, V.; Mottram, P.L.; Plebanski, M. *Methods*, **2006**, 40, 1-9.

(21) Silva, J.M.; Videira, M.; Gaspar, R.; Preat, V.; Florindo, H.F. *J Control Release*, **2013**, 168, 179-199.

(22) Slütter, B.; Soema, P.C.; Ding, Z.; Verheul, R.; Hennink, W.; Jiskoot, W. *J Control Release*, **2010**, 143, 207-214.

(23) Manolova, V.; Flace, A.; Bauer, M.; Schwarz, K.; Saudan, P.; Bachmann, M.F. *Eur J Immunol*, **2008**, 38, 1404-1413.

(24) Rosenthal, J.A.; Chen, L.; Baker, J.L.; Putnam, D.; DeLisa, M.P. *Curr Opin Biotechnol*, **2014**, 28, 51-58.

(25) Reddy, S.T.; van der Vlies, A.J.; Simeoni, E.; Angeli, V.; Randolph, G.J.; O'Neil, C.P.; Lee, L.K.; Swartz, M.A.; Hubbell, J.A. *Nat Biotech*, **2007**, 25, 1159-1164.

(26) Reddy, S.T.; Swartz, M.A.; Hubbell, J.A *Trends Immunol*, **2006**, 27; 573-579.

(27) Duncan, R.; Vicent, M.J *Adv Drug Deliv Rev*, **2010**, 52, 272-282.

(28) Kopeček, J.; Kopečková, P.; Minko, T.; Lu, Z.-R. *Eur J Pharm Biopharm*, **2000**, 50, 61-81.

(29) Rihova, B.; Kovar, M. *Adv Drug Deliv Rev*, **2010**, 62, 184-191.

(30) Torres, A.G.; Gait, M.J. *Trends in Biotech*, **2012**, 30, 185-190.

(31) Yan, Y.; Wang, Y.; Heath, J.K.; Nice, E.C.; Caruso, F. *Adv Mater*, **2011**, 23, 3916-3921.

(32) Qin, Z.; Liu, W.; Li, L.; Guo, L.; Yao, L.; Li, X. *Bioconjug Chem*, **2011**, 22, 1503-1512.

(33) Hugh, M.; Kinns, H.; Mitchell, N.; Astier, Y.; Madathil, R.; Howorka, S. *JACS*, **2007**, 129, 9640-9649.

(34) Shen, Z.; Reznikoff, G.; Dranoff, G.; Rock, K. L *J Immunol*, **1997**, 158, 2723-2730.

(35) Dierendonck, M.; Fierens, K.; De Rycke, R.; Lybaert, L.; Maji, S.; Zhang, Z.; Zhang, Q.; Hoogenboom, R.; Lambrecht, B. N.; Grooten, L.; Remon, J. P.; De Koker, S.; De Geest, B. G. *Adv Funct Mater*, **2014**, 24, 4634-4644.

(36) Boyer, C.; Bulmus, V.; Davis, T.P.; Ladmiral, V.; Liu, J.; Perrier, S. *Chem Rev*, **2009**, 109, 5402-5436.

(37) Fairbanks, B.D.; Gunatillake, P.A.; Meagher, L *Adv Drug Deliv Rev*, **2015**, 91, 141-152.

(38) Heredia, K.L.; Nguyen, T.H.; Chang, C.W.; Bulmus, V.; Davis, T.P.; Maynard, H.D. *Chem Comm*, **2008**, 28, 3245-3247.

(39) Boyer, C.; Liu, J.; Wong, L.; Tippett, M.; Bulmus, V.; Davis, T.P. J. Polym. *Sci Pol Chem,*

2008, 46, 7207-7244.

(40) Wong, L.; Boyer, C.; Jia, Z.; Zareie, H.M.; Davis, T.P.; Bulmus, V.

Biomacromolecules **2008**, *9*, 1934–1944.

(41) Boyer, C.; Bulmus, V.; Davis, T.P. *Macromol Rapid Comm*, **2009**, 30, 493-497.

(42) Boyer, C.; Bulmus, V.; Liu, J.; Davis, T.P.; Stenzel, M.H.; Barner-Kowollik, V. *J Am Chem Soc*, **2007**, *129*, 7145–7154.

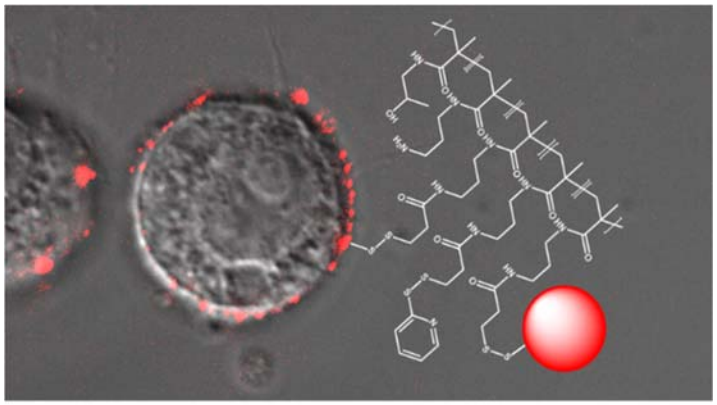

A generic polymer-protein ligation strategy for vaccine delivery

Lien Lybaert,[1] Nane Vanparijs,[1] Kaat Fierens,[2] Martijn Schuijs,[2] Lutz Nuhn,[1] Bart N. Lambrecht.,[2] Bruno G. De Geest[1]*